Acta Crystallographica Section F
Structural Biology and Crystallization Communications
ISSN 1744-3091

Crystallization and X-ray diffraction analysis of dihydropyrimidinase from *Saccharomyces kluyveri*

Doreen Dobritzsch,[a]* Birgit Andersen[b] and Jure Piškur[b]

[a]Department of Medical Biochemistry and Biophysics, Karolinska Institutet, Stockholm, Sweden, and [b]Department of Cell and Organism Biology, Lund University, Lund, Sweden

Correspondence e-mail: doreen.dobritzsch@mbb.ki.se

Received 3 February 2005
Accepted 24 February 2005
Online 12 March 2005

Dihydropyrimidinase (EC 3.5.2.2) catalyzes the second step in the reductive pathway of pyrimidine degradation, the hydrolysis of 5,6-dihydrouracil and 5,6-dihydrothymine to the corresponding N-carbamylated β-amino acids. Crystals of the recombinant enzyme from the yeast *Saccharomyces kluyveri* diffracting to 2.6 Å at a synchrotron-radiation source have been obtained by the hanging-drop vapour-diffusion method. They belong to space group $P2_1$ (unit-cell parameters $a = 91.0$, $b = 73.0$, $c = 161.4$ Å, $\beta = 91.4^\circ$), with one homotetramer per asymmetric unit.

1. Introduction

Dihydropyrimidinase (dihydropyrimidine amidohydrolase, DHPase; EC 3.5.2.2) is the second enzyme in the three-step reductive degradation pathway of uracil and thymine. It catalyzes the reversible hydrolysis of 5,6-dihydrouracil to *N*-carbamyl-β-alanine and of 5,6-dihydrothymine to *N*-carbamyl-β-aminoisobutyrate (Wallach & Grisolia, 1957; Wasternack, 1980). The DHPase reaction and substrates/products mirror those of the third step of *de novo* pyrimidine biosynthesis catalyzed by dihydroorotase (Gojkovic *et al.*, 2003).

The pyrimidine-degrading enzymes are the major cause of the rapid inactivation of 5-fluorouracil and other clinically applied pyrimidine analogues, which are used in the treatment of several common tumours (Wasternack, 1980; Heggie *et al.*, 1987). As a consequence, extremely high doses are applied to increase drug efficiency (Milano & Etienne, 1994), while the accumulated fluorinated degradation products cause severe side effects, especially in the nervous system (Okeda *et al.*, 1990). Furthermore, since the pyrimidine catabolic pathway, together with the *de novo* biosynthetic and the salvage pathways, determines the size of the pyrimidine pool in the cell, it may critically regulate the availability of pyrimidine nucleotides for nucleic acid synthesis during cell proliferation, especially in neoplastic tissue (Ferdinandus *et al.*, 1971). In mammals, it is the only pathway providing β-alanine (Wasternack, 1978). This non-proteinogenic amino acid is thought to possess neurotransmitter function owing to its chemical similarity to γ-aminobutyrate (GABA) and glycine, the two major inhibitory neurotransmitters in the central nervous system (Sandberg & Jacobson, 1981). Genetic defects in pyrimidine catabolism lead to a highly variable clinical phenotype and are usually associated with neurological disorders and high risk of 5-fluorouracil toxicity (van Gennip *et al.*, 1997).

Mammalian DHPase is active in both the liver and kidney (Traut & Loechel, 1984). The enzyme has been purified from rat (Traut & Loechel, 1984; Kikugawa *et al.*, 1994), calf (Kautz & Schnackerz, 1989), pig (Jahnke *et al.*, 1993) and bovine liver (Brooks *et al.*, 1983). Furthermore, gene sequences coding for DHPase from human (Hamajima *et al.*, 1996) and rat liver (Matsuda *et al.*, 1996), from *Caenorhabditis elegans* (Li *et al.*, 1992), *Arabidopsis thaliana*, *Drosophila melanogaster*, *Dictyostelium discoideum* and *Saccharomyces kluyveri* (Gojkovic *et al.*, 2000, 2003) have been cloned from cDNA libraries and partly also expressed as recombinant proteins.

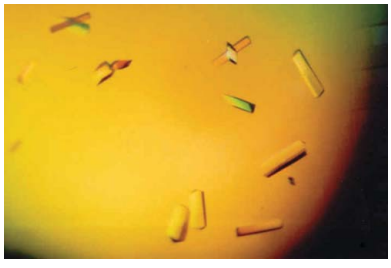

All characterized DHPases are homotetrameric Zn^{2+} metalloenzymes containing four or eight tightly bound Zn ions per molecule of active enzyme (Jahnke *et al.*, 1993; Gojkovic *et al.*, 2003; Kikugawa *et al.*, 1994; Kautz & Schnackerz, 1989; Brooks *et al.*, 1983). The subunit molecular weights range between 56 kDa for slime mould DHPase and 65 kDa for the fruit fly enzyme (Gojkovic *et al.*, 2003).

The pairwise sequence identities of DHPase genes range from 27% for human and yeast DHPase to 94% obtained when the amino-acid sequences of the rat and mouse enzymes are compared. All known DHPases exhibit approximately 25–43% amino-acid sequence identity with hydantoinases, bacterial counterparts of DHPase whose physiological function is most likely not to be connected to reductive degradation of uracil and thymine, since many hydantoinases do not hydrolyze the corresponding dihydropyrimidines (Kim & Kim, 1998; Syldatk *et al.*, 1999). Furthermore, sequence homologies to DHPase have been detected in a number of proteins involved in the development of the nervous system, such as collapsin-response-mediator protein (CRMP; Goshima *et al.*, 1995) and human DHP-related proteins (DRPs; Hamajima *et al.*, 1996).

In this paper, we report the crystallization and preliminary X-ray diffraction data analysis of the first eukaryotic DHPase, the enzyme encoded by PYD2 from the yeast *S. kluyveri*.

2. Material and methods

2.1. Protein purification

The *S. kluyveri* PYD2 gene coding for DHPase was cloned and expressed as His_8-tagged protein using the *Escherichia coli* BL21 strain as described previously (Gojkovic *et al.*, 2000, 2003). The introduction of the tag extends the C-terminus of the polypeptide chain by 18 residues (PGDDDDKHHHHHHHHSGD), yielding a total of 560 amino acids and a molecular weight of 62.3 kDa per subunit. Collected cells were resuspended in buffer *A* [50 m*M* sodium phosphate pH 7.0, 300 m*M* NaCl, 10%(*v*/*v*) glycerol, 1 m*M* dithiothreitol (DTT), 1 n*M* $ZnCl_2$, 0.1 m*M* PMSF with Complete Minus EDTA Protease Inhibitor cocktail tablets from Roche Diagnostics] and disrupted using a French press (4 × 6.9 MPa). After centrifugation at 24 500*g* for 30 min, streptomycin sulfate was added onto the supernatant until a final concentration of 2%(*w*/*v*) was reached. After stirring for 30 min on ice, the suspension was again centrifuged at 24 500*g* for 30 min. To remove the streptomycin salts, the supernatant was applied onto a G-25 column equilibrated and run with buffer *B* (buffer *A* without DTT and protease inhibitors). The desalted protein sample was applied onto a 4.5 ml Ni^{2+}–NTA column (Chelating Sepharose Fast Flow from Amersham Biosciences) equilibrated and washed with buffer *B* with 50 m*M* imidazole. *S. kluyveri* DHPase was eluted with 20 column volumes of a linear gradient of 50–250 m*M* imidazole in buffer *B*. Collected fractions were tested for enzymatic activity by measuring the decrease in absorbance at 225 nm caused by dihydropyrimidine hydrolysis (Kautz & Schnackerz, 1989). Active fractions were pooled and imidazole removed by ammonium sulfate precipitation (the final concentration of ammonium sulfate was equivalent to 70% saturation at 273 K) and resuspension of the protein in buffer *C* [100 m*M* sodium phosphate pH 7.0, 10%(*v*/*v*) glycerol, 1 n*M* $ZnCl_2$]. Finally, the protein was applied onto an S-12 gel-filtration column equilibrated and run with buffer *C*. Active fractions were pooled. For the first crystallization screens the buffer of the protein sample was exchanged to 50 m*M* Tris pH 7.5, 100 m*M* NaCl, 1 m*M* DTT (sample buffer) by repeating steps of centrifugation in Microsep Centrifugal Concentrators (Pall Filtron) at 6000*g* and 277 K for 40 min and addition of sample buffer. Purified *S. kluyveri* DHPase was stored at 253 K for shorter times or at 193 K for long-term storage at a concentration of 20 mg ml^{-1}.

2.2. Crystallization

Initially, sparse-matrix crystallization screens (Hampton Research) were set up at 293 K using 96-well plates and a protein concentration of 2.5 mg ml^{-1} in the drop. The protein crystallized readily (within 1 d) in showers of small crystals under several conditions, all based on polyethylene glycol (PEG) as precipitant. To attempt to obtain larger crystals, the following parameters were varied: buffering agent and buffer pH, precipitant and protein concentration, PEG molecular weight and growth temperature. The best crystals were obtained by hanging-drop vapour diffusion at room temperature with a reservoir solution containing 100 m*M* Tris pH 7.5–8.0, 21–26% PEG 4000. Additive screens (Hampton Research) were performed, resulting in the selection of several additives that seemed to improve crystal size and appearance and were varied in their concentration in follow-up screens. The additive showing the most significant effect was L-cysteine, indicating that a higher concentration of reducing agent was required than the 1 m*M* DTT present in the sample buffer. Thus, varying concentrations of L-cysteine (up to 3 m*M*; higher concentrations lead to formation of cysteine crystals) and of DTT (up to 50 m*M*) were used. Native polyacrylamide gel electrophoresis with DHPase samples containing either 1 or 50 m*M* DTT revealed that the higher concentration of reducing agent leads to the disappearance of a faint band with higher molecular weight that accompanied the main DHPase band. Eventually, crystals of reasonable size for diffraction experiments could be grown. However, during crystal handling it became apparent that the crystals were of rubber-like consistency, explaining their weak X-ray diffraction to a maximum resolution of 7–8 Å.

An entirely new round of screening for crystallization conditions was set up utilizing a variety of other commercially available sparse-matrix and grid screens (Hampton Research). Again, DHPase crystallized readily under a number of conditions which were further explored by variation of the previously mentioned parameters, by addition of known ligands of the enzymes (substrate, product and inhibitors) and by exchange of the sample buffer and the reducing agent.

The best crystals were obtained using vapour diffusion against 19–21% PEG 3350, 0.1 *M* bis-Tris pH 6.5, 0.1 *M* ammonium sulfate. For preparation of the protein solution, DHPase was diluted from an enzyme stock with a concentration of 20 mg ml^{-1} [in 100 m*M* potassium phosphate pH 7.0, 10%(*v*/*v*) glycerol, 1 n*M* $ZnCl_2$] to a protein concentration of 3.5 mg ml^{-1} by addition of 50 m*M* Tris–HCl pH 7.5, 100 m*M* NaCl and 5 m*M* tri(2-carboxyethyl)phosphine hydrochloride (TCEP). It should be noted that these conditions are not very different from those which previously failed to produce well diffracting crystals. We attribute the achieved improvement mostly to the following factors: the presence of low concentrations of phosphate, the presence of additional salt (100 m*M* ammonium sulfate) and possibly also the exchange of the buffering agent. A $ZnCl_2$ effect is unlikely because its concentration of 1 n*M* (originating from the enzyme-purification protocol) is not equimolar with the enzyme concentration of the protein solution used for the crystallization trials. We also noticed that DHPase crystals are sensitive to aging processes: while freshly produced crystals diffract to a resolution better than 2.6 Å, very poor or no diffraction is observed when the tested crystals had been grown more than four weeks prior to data collection. The high concentrations and/or the limited lifetime of DTT used in the earlier crystallization trials might have contributed

to the aging; we did not observe DHPase crystals with a rubber-like consistency after its replacement by TCEP.

The drops consisted of 1.5 µl protein solution and 1.5 µl reservoir solution and were equilibrated against a 1 ml reservoir at room temperature. Crystals appeared within 8 h and reached maximum dimensions of 0.3 × 0.07 × 0.05 mm within 3 d (Fig. 1).

2.3. Data collection and processing

Native data were collected as 0.3° oscillations at 100 K and a wavelength of 1.088 Å at beamline I711 at MAX-lab (Lund, Sweden) using a MAR CCD detector. The crystal-to-detector distance was set to 170 mm and the exposure time per frame to 45 s. Prior to freezing in the nitrogen-gas stream, the crystals were swiftly drawn through a drop of paraffin oil. The data-collection strategy was optimized with the computer program *MOSFLM* (Leslie, 1992). A total of 630 images were collected. All data processing, scaling and truncation was performed using the programs *MOSFLM*, *SCALA* and *TRUNCATE* from the *CCP*4 suite of programs (Collaborative Computational Project, Number 4, 1994).

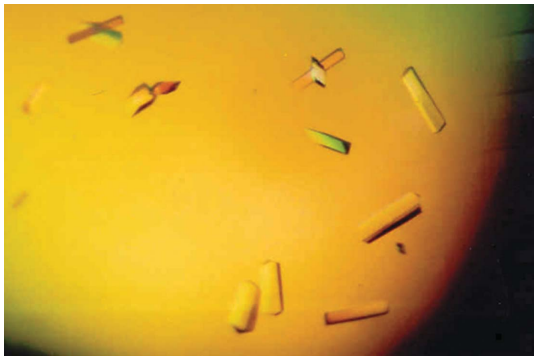

Figure 1
Typical crystals of recombinant DHPase from *S. kluyveri*. The largest dimension is approximately 0.15 mm.

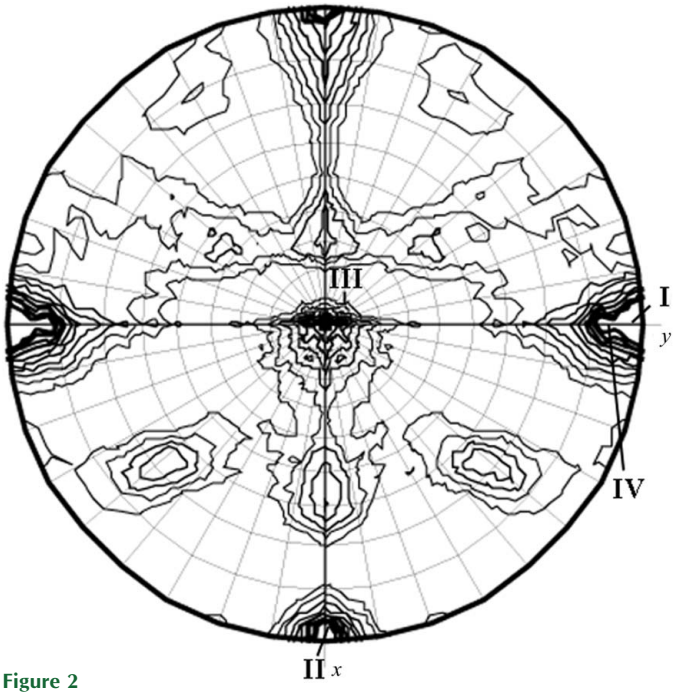

Figure 2
Representation of the $\chi = 180°$ section containing the only significant peaks found in the self-rotation function, which was calculated using a resolution range of 20.0–3.0 Å and a search radius of 30.0 Å. The largest peak, indicated by I in the figure, corresponds to the crystallographic twofold axis. The location of the three next highest peaks II, III and IV suggests that the asymmetric unit of the DHPase crystals contains one homotetramer in which the subunits are related by 222 symmetry and with the three non-crystallographic symmetry axes lying almost parallel to the *x*, *y* and *z* axis, respectively.

Table 1
Diffraction, data-collection and reduction statistics.

Values in parentheses are for the highest resolution shell (2.74–2.60 Å).

Wavelength (Å)	1.088
Space group	$P2_1$
Unit-cell parameters (Å, °)	a = 91.0, b = 73.0, c = 161.4, β = 91.4
Resolution limits (Å)	40.0–2.6
No. of reflections	170159
No. of unique reflections	60029
R_{sym} (%)	11.9 (26.8)
Mean $I/\sigma(I)$	9.6 (3.1)
Completeness (%)	91.7 (89.3)
Multiplicity	2.8 (2.7)

3. Results

Although the autoindexing routine predicted a primitive orthorhombic cell, the crystallographic data could not be scaled in Laue class *mmm*. Instead, the crystals of DHPase belong to the monoclinic space group $P2_1$, with unit-cell parameters a = 91.0, b = 73.0, c = 161.4 Å, β = 91.4°. A self-rotation function calculated with the program *MOLREP* (Vagin & Teplyakov, 1997) is shown in Fig. 2. The Patterson synthesis did not produce any strong peaks.

DHPase crystals generally exhibit high mosaicity (>1°) and weak X-ray diffraction, necessitating small oscillation angles and longer exposure times. Although the crystals diffracted to 2.3 Å, integration statistics steeply declined beyond 2.6 Å. The R_{sym} at 2.6 Å was 11.9%, with the data 91.7% complete. Data statistics are given in Table 1. The value of the Matthews coefficient (Matthews, 1968) is 2.2 Å^3 Da^{-1} assuming four polypeptide chains in the asymmetric unit, which corresponds to a solvent content of 42.3%.

Molecular-replacement trials were carried out using *EPMR* (Kissinger *et al.*, 1999) with a polyalanine model of the structure of *Burkholderia pickettii* D-hydantoinase (PDB code 1nfg; Xu *et al.*, 2003) as a search model. Solutions for molecules *A* and *B* were obtained with the first run and showed convincing crystal packing, with the formation of an extended β-sheet between the two molecules and without any serious clashes. The search for the other two molecules was not similarly straightforward; several runs with changed search parameters also remained unsuccessful. Eventually, replacement of the original monomeric search model by the dimer of the already found solutions yielded the correct orientation and position of the third molecule in the asymmetric unit. Those of the fourth needed to be adjusted by the application of non-crystallographic symmetry, because the positional errors of the (unrefined) dimeric search model had amounted to a modest shift and some clashes with another subunit. Preliminary density maps suggest that the correct solution had been found and model building and refinement of the structure are in progress.

This work was supported by grants from the Swedish Research Council, the Foundations Lars Hiertas Minne and Åke Wibergs Stiftelse, Karolinska Institutes Research Foundation and the Danish Research Council. We acknowledge access to synchrotron radiation and would like to thank the staff at the European Synchrotron

Radiation Facility, Grenoble and MAX-lab, Lund for their assistance with data collection.

References

Brooks, K. P., Jones, E. A., Kim, B.-D. & Sander, E. G. (1983). *Arch. Biochem. Biophys.* **226**, 469–483.

Collaborative Computational Project, Number 4 (1994). *Acta Cryst.* D**50**, 760–763.

Ferdinandus, J. A., Morris, H. P. & Weber, G. (1971). *Cancer Res.* **31**, 550–556.

Gennip, A. H. van, Abeling, N. G. G. M., Vreken, P. & van Kuilenburg, A. B. P. (1997). *J. Inherit. Metab. Dis.* **20**, 203–213.

Gojkovic, Z., Jahnke, K., Schnackerz, K. D. & Piškur, J. (2000). *J. Mol. Biol.* **295**, 1073-1087.

Gojkovic, Z., Rislund, L., Andersen, B., Sandrini, M. P. B., Cook, P. F., Schnackerz, K. D. & Piškur, J. (2003). *Nucleic Acids Res.* **31**, 1683–1692.

Goshima, Y., Nakamura, F., Strittmatter, P. & Strittmatter, S. M. (1995). *Nature (London)*, **376**, 509–514.

Hamajima, N., Matsuda, K., Sakata, S., Tamaki, N., Sasaki, M. & Nonaka, M. (1996). *Gene*, **180**, 157–163.

Heggie, G. D., Sommadossi, J.-P., Cross, D. S., Huster, W. J. & Diasio, R. B. (1987). *Cancer Res.* **47**, 2203–2206.

Jahnke, K., Podschun, B., Schnackerz, K. D., Kautz, J. & Cook, P. F. (1993). *Biochemistry*, **32**, 5160–5166.

Kautz, J. & Schnackerz, K. D. (1989). *Eur. J. Biochem.* **181**, 431–435.

Kikugawa, M., Kaneko, M., Fujimoto-Sakata, S., Maeda, M., Kawasaki, K., Takagi, T. & Tamaki, N. (1994). *Eur. J. Biochem.* **219**, 393–399.

Kim, G. J. & Kim, H. S. (1998). *Biochem. J.* **330**, 295–302.

Kissinger, C. R., Gehlhaar, D. K. & Fogel, D. B. (1999). *Acta Cryst.* D**55**, 484–491.

Leslie, A. G. W. (1992). *Jnt CCP4/ESF–EACBM Newsl. Protein Crystallogr.* **26**.

Li, W., Herman, R. K. & Shaw, J. E. (1992). *Genetics*, **132**, 675–689.

Matsuda, K., Sakata, S., Kaneko, M., Hamajima, N., Nonaka, M., Sasaki, M. & Tamaki, N. (1996). *Biochim. Biophys. Acta*, **1307**, 140–144.

Matthews, B. W. (1968). *J. Mol. Biol.* **33**, 491–497.

Milano, G. & Etienne, M.-C. (1994). *Pharmacogenetics*, **4**, 301–306.

Okeda, R., Shibutani, M., Matsuo, T., Kuroiwa, T., Shimokawa, R. & Tajima, T. (1990). *Acta Neuropathol.* **81**, 66–73.

Traut, T. & Loechel, S. (1984). *Biochemistry*, **23**, 2522–2539.

Sandberg, M. & Jacobson, I. (1981). *J. Neurochem.* **37**, 1353–1356.

Syldatk, C., May, O., Altenbuchner, J., Mattes, R. & Siemann, M. (1999). *Appl. Microbiol. Biotechnol.* **51**, 293–309.

Vagin, A. & Teplyakov, A. (1997). *J. Appl. Cryst.* **30**, 1022–1025.

Wallach, D. P. & Grisolia, S. (1957). *J. Biol. Chem.* **226**, 277–288.

Wasternack, C. (1978). *Biochem. Physiol. Pflanz.* **173**, 371–403.

Wasternack, C. (1980). *Pharmacol. Ther.* **8**, 629–651.

Xu, Z., Liu, Y., Yang, Y., Jiang, W., Arnold, E. & Ding, J. (2003). *J. Bacteriol.* **185**, 4038–4049.